Current Biology 19, 1320–1326, August 11, 2009 ©2009 Elsevier Ltd All rights reserved DOI 10.1016/j.cub.2009.06.046

Report

The Mammalian Cos2 Homolog Kif7 Plays an Essential Role in Modulating Hh Signal Transduction during Development

Setsu Endoh-Yamagami,[1] Marie Evangelista,[1] Deanna Wilson,[1] Xiaohui Wen,[1] Jan-Willem Theunissen,[1] Khanhky Phamluong,[1] Matti Davis,[1] Suzie J. Scales,[1] Mark J. Solloway,[1] Frederic J. de Sauvage,[1] and Andrew S. Peterson[1,*]

[1]Department of Molecular Biology, Genentech, Inc., 1 DNA Way, South San Francisco, CA 94080, USA

Summary

The Hedgehog (Hh) signaling pathway regulates development in animals ranging from flies to humans. Although its framework is conserved, differences in pathway components have been reported [1–4]. A kinesin-like protein, Costal2 (Cos2), plays a central role in the Hh pathway in flies [3, 5]. Knockdown of a zebrafish homolog of Cos2, Kif7, results in ectopic Hh signaling, suggesting that Kif7 acts primarily as a negative regulator of Hh signal transduction [6]. However, in vitro analysis of the function of mammalian Kif7 and the closely related Kif27 has led to the conclusion that neither protein has a role in Hh signaling [4]. Using *Kif7* knockout mice, we demonstrate that mouse Kif7, like its zebrafish and *Drosophila* homologs, plays a role in transducing the Hh signal. We show that Kif7 accumulates at the distal tip of the primary cilia in a Hh-dependent manner. We also demonstrate a requirement for Kif7 in the efficient localization of Gli3 to cilia in response to Hh and for the processing of Gli3 to its repressor form. These results suggest a role for Kif7 in coordinating Hh signal transduction at the tip of cilia and preventing Gli3 cleavage into a repressor form in the presence of Hh.

Results and Discussion

We generated a mouse knockout of Kif7 to analyze its role in the Hedgehog (Hh) pathway (Figure S1, available online). Homozygous mutant embryos have characteristic defects reminiscent of *Gli3* mutants [7]: preaxial polydactyly, exencephaly, and microphthalmia (Figures 1A–1I). Hh ligands work through two membrane proteins, Patched (Ptch) and Smoothened (Smo), and regulate the activities of the transcription factors Cubitus interruptus (Ci) in flies and Gli1, 2, and 3 in vertebrates. These transcription factors act as transcriptional activators in their full-length form and function as transcriptional repressors if processed by proteolytic cleavage events, which are inhibited by Hh. Although Gli1 and Gli2 act primarily as transcriptional activators, the major transcriptional repressor activity is carried by Gli3. The parallel phenotypes of $Gli3^{-/-}$ and $Kif7^{-/-}$ suggest a role for Kif7 in the Sonic Hedgehog (Shh) signaling pathway. To examine this in more detail, we crossed $Kif7^{-/-}$ mice with a *Ptch-LacZ* reporter line [8] to reveal the pattern of Shh signaling in the spinal cord, a tissue where the role and pattern of Shh signaling has been well characterized. In wild-type (WT) embryos at 10.5 days of gestation (E10.5), β-galactosidase is expressed at high levels ventrally, falling off rapidly dorsally in a steep gradient of response to Shh that emanates from the notochord and floor plate (Figure 1J). In $Kif7^{-/-}$ mutants, the gradient is less steep, with β-galactosidase positive cells expanded toward the dorsal portion of the spinal cord and with a reduction in the peak levels of the most ventral portion of the neural tube as well (Figure 1K, Figure S2A). The dorsal extension of the β-galactosidase staining is consistent with the suggestion from the gross phenotype that there is a loss of Gli3 function; however, the reduction in β-galactosidase expression in the ventral spinal cord suggests a broader defect in Shh signaling.

To examine in more detail the idea that Shh signaling is defective in the *Kif7* mutant, we analyzed the expression of Shh and Shh-induced patterning in the embryo, focusing on the spinal cord and limb where the role of Shh has been well established [9, 10]. Expression of Shh in the notochord and floor plate creates a ventral-to-dorsal gradient of Shh and induces a parallel gradient of Gli activator activity in the neural tube. Shh also induces a gradient of Gli repressor activity that is oriented in the opposite direction to the Shh gradient with high dorsal levels of repressor and low levels ventrally. The balance between Gli activator and repressor activities is important in establishing the dorsal-ventral pattern of the neural tube. Examination of the spinal cord of embryos at both E9.5 (Figures 2A–2H, Figure S2B) and E10.5 (Figure S2C) at the rostral and caudal levels showed consistent defects. The expression of Shh in the notochord and floor plate was reduced to a variable extent in mutant animals with some showing wild-type levels of Shh expression and others showing a significant reduction (e.g., Figure 2B; see also Figure S2B). Reduction in Shh expression in the notochord correlated with reduction of Shh and FoxA2 expression in the floor plate (compare Figures 2A and 2C with Figures 2B and 2D; see also Figure S2B). Concomitant with reduction in FoxA2 expression is an expansion of the V3 interneuron progenitor domain, marked by Nkx2.2 expression, to fill the ventral midline. Reduced ventral cell types in the mutant suggest the possibility that Kif7 is required for Shh pathway activation, but the reduced Shh expression in the notochord and floor plate prevents us from drawing any such conclusion. More dorsally, motor neuron (MN) progenitors expressing Olig2 are expanded and $Olig2^{+}$ cells are intermixed with V0–V2 progenitor cells expressing high levels of Pax6 in $Kif7^{-/-}$ mutants (Figure 2E–2H). Both the expanded and intermingled expression of Olig2 are observed in Gli3 mutants in combination with *Smo* or *Gli2* mutations [11, 12], indicating that Gli3 repressor function is reduced in $Kif7^{-/-}$ mutants. The reduction in notochordal Shh expression and the apparent reduction in Gli3 repressor activity both contribute to the altered gradient of *Ptch-LacZ* expression observed in mutant embryos (Figures 1J and 1K). Tay et al. reported that zebrafish Kif7 morpholino knockdown causes ectopic Hh signaling in the somites and the ventral neural tube, and they indicated that Kif7 functions principally as a repressor of Hh signal transduction similar to the role of Costal2 (Cos2) in flies [6]. Our observation that mouse Kif7 is required for the transcriptional repression activity of the Shh pathway is consistent with these previous observations and

*Correspondence: peterson.andrew@gene.com

A

Stage	Polydactyly	Microphthalmia	Exencephaly
15.5-18.5 dpc	17/22 (77%)	17/22 (77%)	2/22 (9%)

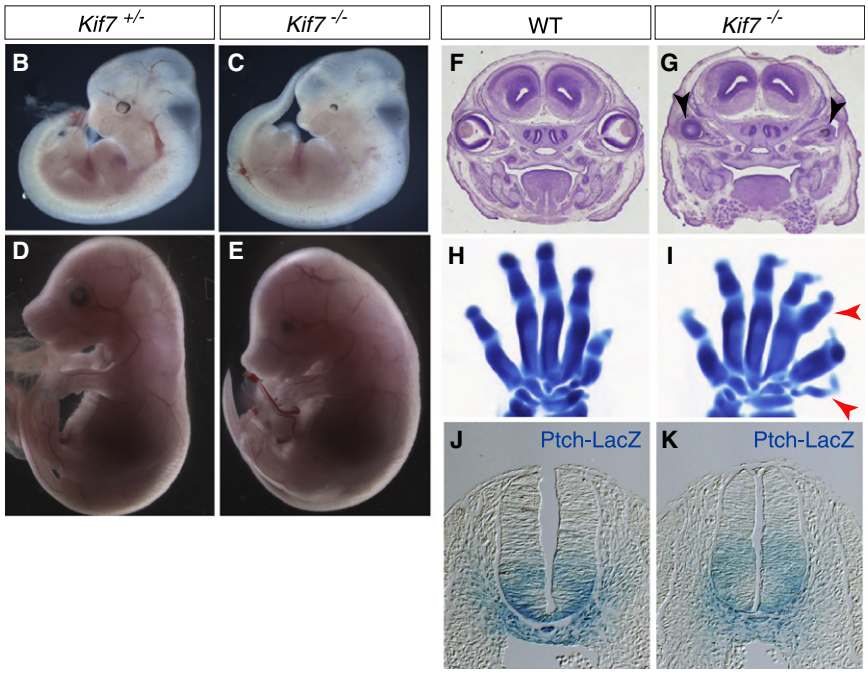

Figure 1. The *Kif7* Mutant Phenotype Implies a Role in the Hh Signaling Pathway

(A) Incidence of phenotypic parameters in *Kif7*$^{-/-}$ mutant embryos.

(B–E) Gross appearance of E11.5 (B and C) and E16.5 (D and E) embryos. An abnormally smaller eye (microphthalmia) is observed in the *Kif7*$^{-/-}$ mutant. Note that at late stages of embryonic development the mutant often shows edema, which is not illustrated here (E).

(F and G) Coronal sections through heads of E15.5 embryos show microphthalmia (black arrowheads) in *Kif7*$^{-/-}$ mutant embryos.

(H and I) Alcian-blue-stained skeletal preps of left front paws from E15.5 embryos illustrate the preaxial polydactyly (red arrowheads) in the mutant.

(J and K) X-gal-stained sections of spinal cord, at the level of the hindlimb, from E10.5 *Ptch-LacZ*$^{+/-}$; *Kif7*$^{+/+}$ and *Ptch-LacZ*$^{+/-}$; *Kif7*$^{-/-}$ embryos. Reduced ventral staining and a dorsally expanded extent of staining are observed in *Kif7*$^{-/-}$ embryos.

suggests that the function of Kif7 and Cos2 is conserved from flies to fish and mammals.

Shh plays an important role in patterning the developing limb. Gli3 repressor function has a particularly critical role in determining the final structure of the limb, but the activity of both activator and repressor can be seen in the pattern of gene expression during early development [10, 13]. To examine the role of Shh signaling defects in the polydactyly of *Kif7*$^{-/-}$ mutants, we looked at a set of markers that reveal the activity of Gli activator and Gli repressor function. In the posterior portion of the limb, expression of *Shh*, *Gli1*, and *Ptch1* are not reduced by loss of Kif7 (Figures 2I and 2J, Figure S2D), indicating that Kif7 does not play a critical role in the transcriptional activation events downstream of Shh. The expression of *Gremlin* (Figures 2K–2N) and *HoxD13* (Figure S2D) on the other hand is expanded anteriorly. Both of these genes are targets of repression by Gli3 [13, 14], indicating that a loss of Gli3 repressor function is the likely reason for polydactyly in the knockout.

Patterning defects in both the spinal cord and limb bud of *Kif7*$^{-/-}$ embryos point toward a role for Kif7 in the formation of Gli3 repressor. To test this supposition directly, we examined the proteolytic processing of Gli3 in mutant embryos. Gli3 is synthesized as a 190 kDa full-length precursor. A Shh-inhibited cleavage event produces an 83 kDa fragment that functions as a transcriptional repressor [15]. In *Kif7* mutant embryos, substantially less repressor is formed (Figure 3A), indicating that Kif7 is required for the processing of Gli3 as Cos2 is in *Drosophila* [5, 16, 17]. The requirement for Kif7 in the Gli3 processing substantiates directly the results provided by the patterning defects in the spinal cord and limb bud.

Although patterning of the limb bud does not provide clear evidence that Kif7 is required for Gli-mediated transcriptional activation, we reasoned that a more quantitative in vitro assay might reveal such a role. Fibroblasts prepared from *Kif7*$^{-/-}$ embryos (*Kif7*$^{-/-}$ mouse embryonic fibroblasts [MEFs]) were established in culture, and the ability of exogenously added Shh to induce *Gli1* and *Ptch1* expression was measured (Figure 3B). *Kif7*$^{-/-}$ MEFs showed induction of *Gli1* and *Ptch1* mRNA comparable to that seen with wild-type MEFs, again suggesting that Kif7 does not play a critical role in Gli-mediated transcriptional activation. In the same experiments, expression of *Kif7* and its close relative, *Kif27*, was examined (Figure S3A). We confirmed that *Kif7* expression was not detected in the *Kif7*$^{-/-}$ MEFs and found that *Kif27* expression did not change in the presence or absence of *Kif7* (Figure S3A). Although we cannot rule out functional redundancy between Kif7 and Kif27, compensatory induction of *Kif27* expression does not occur.

Although we did not see any significant impairment in Shh-mediated target gene induction in *Kif7*$^{-/-}$ MEFs, we observed a slight increase in target expression in the absence of Shh (Figure 3B). A similar derepression of Hh signaling is produced by loss of Kif7 expression in zebrafish, and the pathway is further derepressed in this species by the simultaneous loss of Sufu, a negative regulator in the Hh pathway [6]. To explore the possibility that functional interaction between Kif7 and Sufu occurs in mammals, we knocked down the expression of Sufu in both WT and *Kif7*$^{-/-}$ MEFs. Indeed, knockdown of Sufu caused an apparently synergistic derepression of target gene expression in the absence of Shh treatment (Figure 3C, Figure S3B). These results indicate a collaborative effect of mouse Kif7 and Sufu in repressing the Hh pathway, as has been seen in zebrafish and *Drosophila* [3, 5, 6, 18].

The role of Cos2 in Hh signal transduction involves interaction with Smo, Ci, Fused, and Sufu. Previous studies on the role of zebrafish Kif7 showed physical interaction between Kif7 and Gli1 [6]. Given this prior work and the *Gli3* mutant-like phenotype of the mouse *Kif7* knockout, we focused our efforts on a potential interaction with Gli transcription factors and Gli3 in particular. We first generated an NIH 3T3 cell line

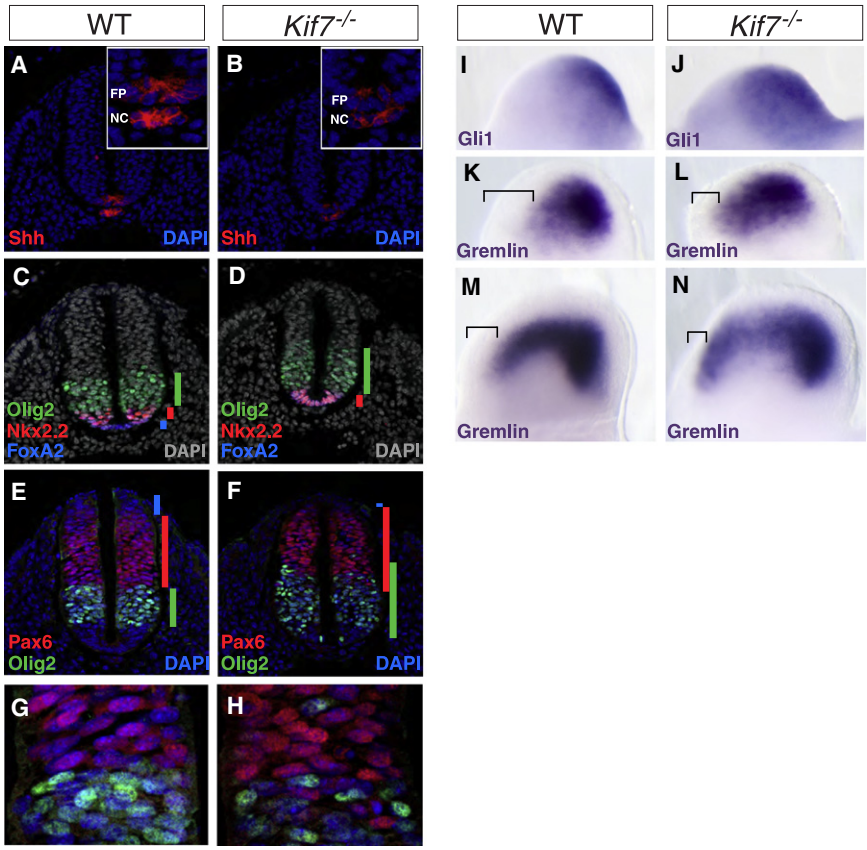

Figure 2. Spinal Cord and Limb Bud Patterning Defects Indicate a Loss of Gli3 Repressor Activity

(A–F) Expression of marker genes visualized by immunofluoresence in WT and mutant E9.5 spinal cord at the level of the forelimb.

(A and B) Shh expression. The insets show higher-resolution images of the notochord (NC) and floor plate (FP) region of the same sections shown in the main panels.

(C and D) Olig2, Nkx2.2, and FoxA2 expression. The FoxA2^{+} floor plate region is diminished or absent in the mutant, and Nkx2.2 expression instead fills the ventral midline.

(E and F) Pax6 and Olig2 expression. Olig2 is expanded ventrally and dorsally in the mutant. The wild-type cells that are strongly Pax6 positive do not mix with the neighboring Olig2^{+} population forming a clear boundary, whereas in the mutant, extensive interdigitation of the two cell-types occurs. Vertical bars show the extent of staining.

(G and H) Higher-magnification images of the Pax6-Olig2 boundary region. Note misplaced cells in the mutant.

(I–N) Expression of marker genes visualized by whole-mount in situ hybridization using Alkaline phosphatase for detection. The dorsal face of the right forelimb is shown in each case with anterior to the left and posterior to the right.

(I and J) *Gli1* expression is not reduced in *Kif7*$^{-/-}$ embryos. *Gli1* expression is dependent upon transcriptional activation downstream of Shh.

(K–N) *Gremlin* expression in 27 (K and L) and 30 (M and N) somite stage limb buds. The expression of *Gremlin* is expanded to the anterior margin of the limb bud at both stages. Brackets indicate the anterior domain that is free of Gremlin expression.

stably expressing Kif7-GFP and transfected these cells with a full-length myc-tagged Gli3 construct. Extracts immunoprecipitated with anti-GFP antibody but not IgG control associated with both full-length Gli3 and the 83 kDa cleavage fragment, indicating that Kif7 interacts with Gli3 (Figure 3D). Because the 83 kDa fragment is derived from the amino-terminal portion of Gli3, we expected that the binding site resides in the amino-terminal region of Gli3 and examined a potential interaction with this domain more directly by using constructs that expressed either myc-tagged amino-terminal or carboxy-terminal fragments of Gli3. Indeed, the amino-terminal but not the carboxy-terminal fragment is associated with Kif7 (Figure 3E). We determined whether Kif7 interacts with Gli1 and Gli2 as well as Gli3 and found that Kif7 physically interacts with both of them (Figure 3F), consistent with the previously reported interaction between Kif7 and Gli1 in zebrafish [6]. Because it is known that Cos2 forms a tetrameric complex with Fused, Ci, and Su(fu) in flies [19], we asked whether there is also an interaction between Kif7 and Sufu, and we also detected interaction between these two pathway components (Figure 3F). We also found that Kif7 can bind to Smo in an in vitro assay (Figure S3C) just as Cos2 binds to *Drosophila* Smo (dSmo) [20, 21]. Cos2 binds to the carboxy-terminal tail of dSmo [20, 21], and we detected interaction between Kif7 and the Smo tail (Figure S3C). Smo lacking its carboxy-terminal tail, however, retains binding to Kif7 (Figure S3C), making the requirements for specific binding unclear, but suggesting that there is more than one binding site in Smo for Kif7. Varjosalo et al. did not detect interaction between the cargo domain of Kif7 and Smo, whereas we used the full-length protein [4], suggesting that binding involves other domains of Kif7. The interaction of Kif7 with Gli proteins, Sufu, and Smo all support a conserved function of Kif7 and Cos2 from flies to fish and mammals.

The association of Kif7 with Gli proteins, Sufu, and Smo suggested that at least some aspects of Kif7 role in Hh signal transduction are conserved vis-à-vis Cos2. A significant divergence in the signaling pathway between flies and vertebrates occurs at events that take place immediately downstream of Hh binding to Ptch1, events that in flies involve Cos2 [1, 2]. In vertebrates, these events involve translocation of Smo and Gli proteins to primary cilia [22, 23]. Cilia do not play a role in Hh signaling in flies, although Smo and Ci are translocated to the plasma membrane in a Hh-dependent manner. To elucidate the mechanism whereby Kif7 functions in Shh signaling, we carried out a series of experiments examining the potential for cilia localization of Kif7 with respect to Smo and Gli3. We first tested the possibility that Kif7 is localized to the cilia in a Shh-dependent fashion. Careful examination of the NIH 3T3 cells that express Kif7-GFP revealed that the presence of Kif7 at the tip of cilia was significantly increased upon stimulation with exogenous Shh (Figures 4A–4C). Costaining for endogenous Gli3 confirmed its Shh-dependent accumulation (Figures 4A–4C, Figure S4; X.W. and S.J.C., unpublished data) in a pattern that paralleled the localization of Kif7. Given the Kif7-Gli3 association detected by immunoprecipitation, we hypothesized that Kif7 might be required for Gli3 accumulation within cilia. To test this hypothesis, we examined the localization of endogenous Gli3 in WT and *Kif7*$^{-/-}$ MEFs. In *Kif7*$^{-/-}$ MEFs, the level of Shh-induced accumulation of Gli3 is

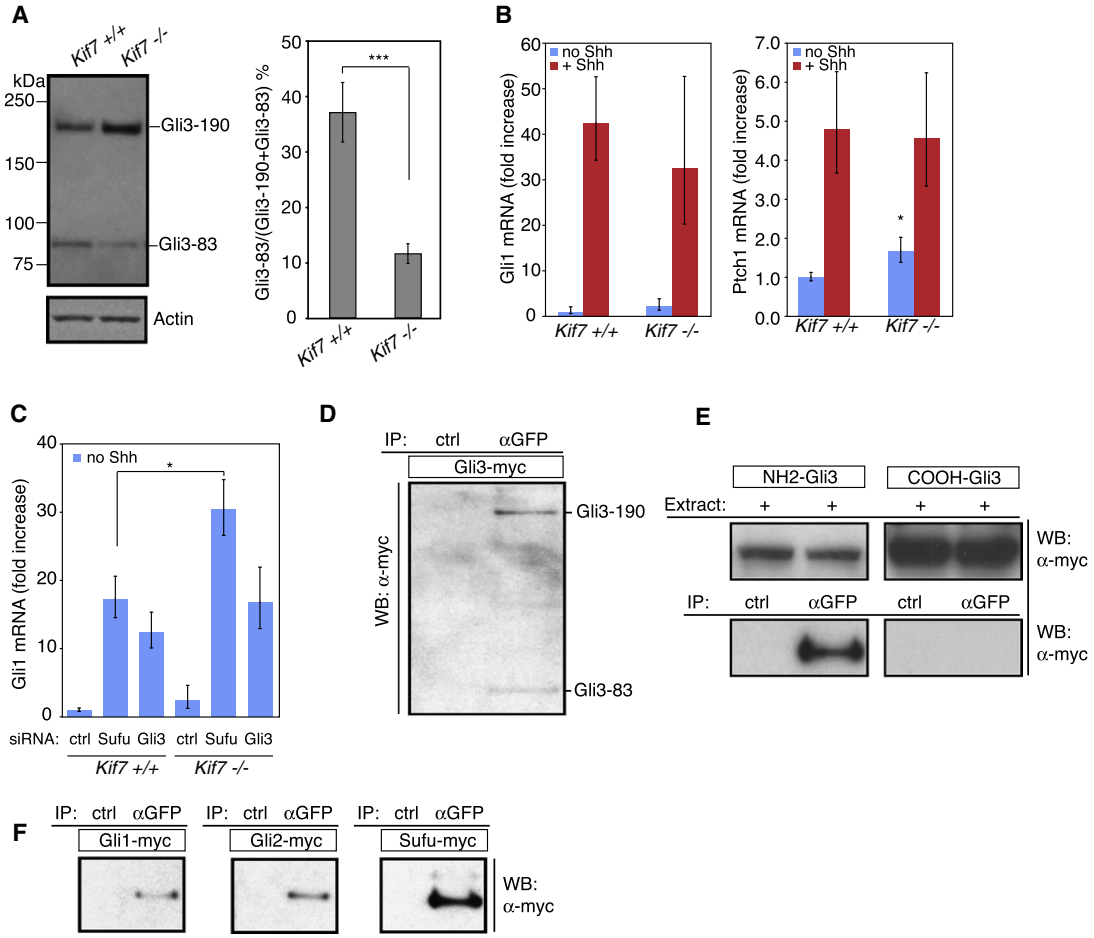

Figure 3. Kif7 Is a Negative Regulator of the Hh Pathway

(A) Western-blot analysis of Gli3 processing with extracts from individual E10.5 embryos and Gli3 monoclonal antibody. Lanes of representative embryos are shown. The band intensities of the 83 kDa (Gli3-83) and 190 kDa (Gli3-190) fragments were measured in each lane (*Kif7*$^{+/+}$, n = 4; *Kif7*$^{-/-}$, n = 5). The mean and standard deviation (SD) of the amount of Gli3-83 as a percentage of the total amount of Gli3 (Gli3-190 + Gli3-83) are graphed. *** indicates p = 1.97E-05 (t test).

(B) Expression of *Gli1* and *Ptch1* in WT and *Kif7*$^{-/-}$ MEFs. Confluent cultures of fibroblast cell lines from WT and *Kif7*$^{-/-}$ embryos (MEFs) were either untreated or exposed to 200 ng/ml of Shh for 24 hr. The expression of *Gli1* and *Ptch1* mRNA was normalized to the *RPL19* housekeeping gene ($2^{-\Delta Ct}$) and calculated relative to controls ($2^{-\Delta\Delta Ct}$) by real-time qRT-PCR. The mean and SD of three independent experiments using three different cell lines are graphed. Statistical analysis was performed with ΔCt values. *Kif7*$^{-/-}$ MEFs showed *Gli1* and *Ptch1* mRNA induction by Shh at the comparable levels to wild-type MEFs (p = 0.43, and 0.84, respectively, with t test). * indicates p = 0.016 (*Kif7*$^{+/+}$ versus *Kif7*$^{-/-}$ without Hh, t test).

(C) Effect of Sufu knockdown in *Kif7*$^{-/-}$ MEFs. WT and *Kif7*$^{-/-}$ MEFs were transfected with control (ctrl), Sufu, and Gli3 siRNA, and relative *Gli1* mRNA levels were examined. Gli3 siRNA was used as a positive control, showing increased *Gli1* induction by Gli3 knockdown. Simultaneous loss of Kif7 and Sufu showed higher *Gli1* expression compared to individual loss. The mean and SD of three independent experiments with three different cell lines are graphed. * indicates p = 0.011 (t test).

(D) Western-blot detection of myc-tagged Gli3 association with GFP-Kif7 immunoprecipitated from a Kif7-GFP NIH 3T3 stable cell extract with anti-GFP antibody. IgG was used as a negative control.

(E) Immunoprecipitation experiments were similarly carried out in cells expressing truncated expression constructs. NH2-Gli3 and COOH-Gli3 contain 2–676 aa and 780–1548 aa of human Gli3, respectively.

(F) Immunoprecipitation experiments were similarly carried out in cells expressing myc-tagged Gli1, Gli2, or Sufu.

substantially reduced, indicating that Kif7 is required for efficient Gli3 localization at the ciliary tip (Figures 4D–4F). *Kif7*$^{-/-}$ MEF cells often show Gli3 accumulation in the midportion of cilia or spread from the tip toward the base of cilia in response to Shh, a pattern that is rarely observed in WT MEFs (Figure S5A). Examination of the level of Gli2 accumulation in the cilia in response to Shh showed that it is also affected by *Kif7* knockout (Figures S5B and S5C).

Because ciliary localization of Sufu has been reported [23] and Kif7 appears to cooperate with Sufu in maintaining repression of the pathway in the absence of Shh (Figures 3C and 3F), we asked whether Kif7 is also required for Sufu localization (Figure S6). In NIH 3T3 cells that stably express GFP-Sufu, we found that Sufu is present at the tip of cilia in the absence of Hh (Figures S6A and S6B). Importantly, localization of Sufu to the ciliary tip in the absence of Hh is not affected by Kif7 siRNA knockdown (Figures S6A–S6C). Furthermore, although Hh treatment substantially increases the accumulation of Kif7, Gli2, and Gli3 at the distal tip of primary cilia (Figures 4A–4C, Figure S5), Hh only mildly increases the levels of Sufu at the distal tip (Figures S6A–S6B). Although we confirmed the efficiency of the knockdown at the protein level (Figure S6C), we cannot exclude the possibility that the knockdown does not result in complete Kif7 inactivation. Nonetheless, these results support

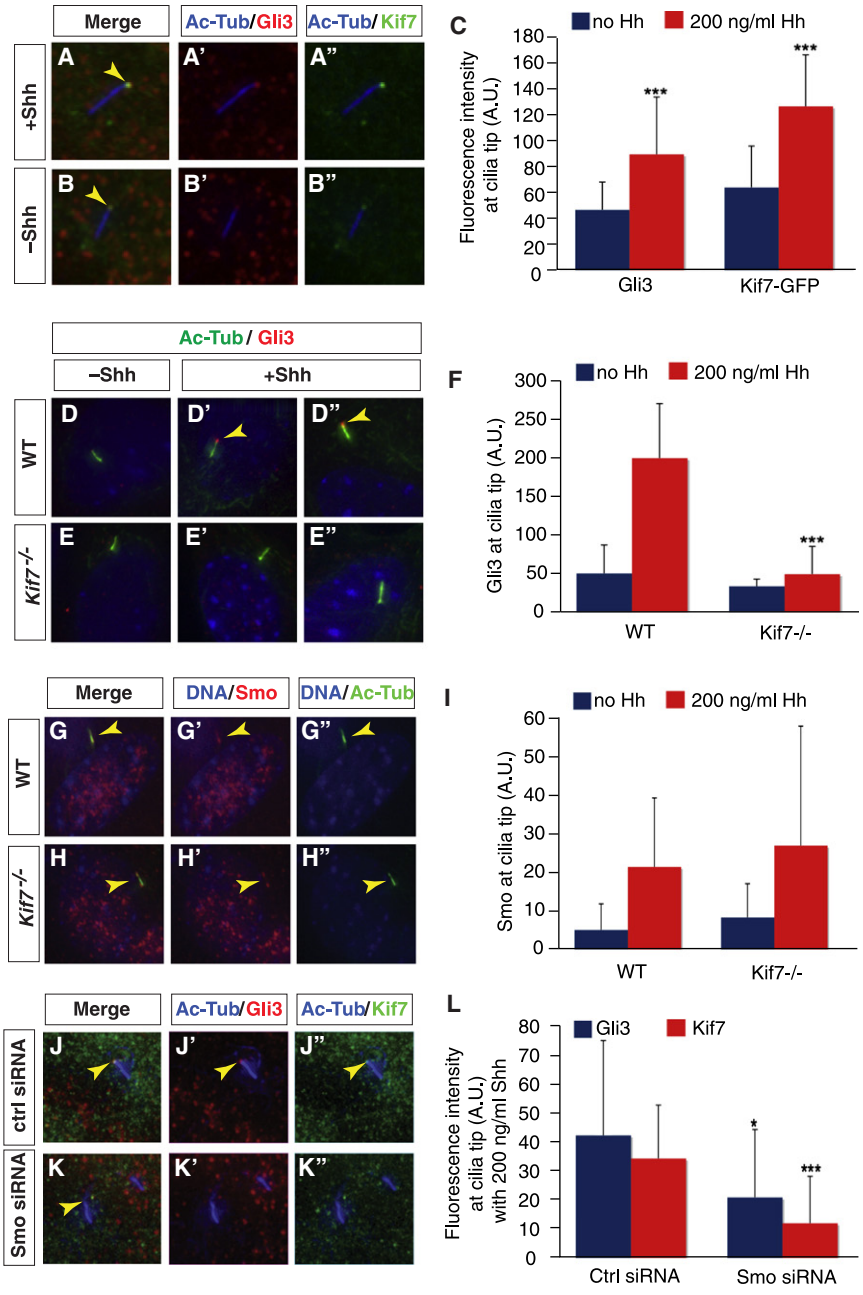

Figure 4. Hh-Dependent Accumulation of Kif7 in the Primary Cilia Functions Downstream of Smo to Mediate Gli3 Localization

(A–C) Kif7 and Gli3 accumulate at the distal tip of the primary cilia in response to stimulation of Kif7-GFP NIH 3T3 cells with Shh.

(A–B″) Representative cells stained with antibodies against acetylated-tubulin to label the cilial axoneme, GFP to visualize Kif7, and Gli3. Kif7 and Gli3 show increased cilia localization upon the addition of Shh ligand.

(C) Quantification of (A)–(B″) with ImageJ software. The mean and SD of the fluorescent signal at the tip of the cilia from at least 50 cells per treatment group is graphed and is expressed in arbitrary units. *** indicates a significant difference between Shh-treated and untreated cells ($p < 0.001$).

(D–F) Kif7 is required for the accumulation of Gli3 in cilia.

(D–E″) WT or *Kif7*$^{-/-}$ MEFs treated with Shh ligand and stained with antibodies to visualize the primary cilia and endogenous Gli3.

(F) Quantification of (D)–(E″) with at least 20 cells per treatment group. *** indicates a significant difference between Shh-treated and untreated cells ($p < 0.001$).

(G–I) Shh-dependent localization of Smo to the cilia does not require Kif7.

(G–H″) WT or *Kif7*$^{-/-}$ MEFs treated with Shh ligand and stained with antibodies to visualize the primary cilia and endogenous Smo.

(I) Quantification of (G)–(H″) with at least 20 cells per treatment group.

(J–L) Smo is required for Kif7 and Gli3 localization to the cilia.

(J–K″) Kif7-GFP cells transfected with nontargeting control or Smo siRNA, treated with Shh, and stained to visualize the primary cilia, Kif7, and endogenous Gli3.

(L) Quantification of (J–K″) with at least 20 cells per treatment group. * and *** indicate significant differences between control and Smo siRNA-treated cells (* indicates $p < 0.05$ and *** indicates $p < 0.001$).

The mean and SD are graphed (C, F, I, and L).

a model in which Kif7 is specifically required for accumulation of the Gli proteins at the distal tip of primary cilia upon activation of Hh signaling. Although cilia are required for both repressor and activator functions of Gli proteins [23–26], it was recently reported that the inhibitory function of Sufu in Hh signaling does not require cilia [27] and the cellular location at which Kif7 and Sufu functionally interact remains to be addressed.

To place Kif7 relative to Smo in the hierarchy of Shh-dependent cilia localization events, we first determined whether Kif7 is required for Smo accumulation. *Kif7*$^{-/-}$ MEFs show robust accumulation of endogenous Smo upon treatment with Shh (Figures 4G–4I, Figure S7), indicating that Kif7 is not involved in the Hh-regulated translocation of Smo to the cilia. In contrast, we found that Smo is required for the accumulation of Kif7 within cilia. Knockdown of Smo via siRNA prevented the localization of both Kif7 and Gli3 to the cilia upon Shh treatment (Figures 4J–4L). These results clearly place Kif7 downstream of Smo and upstream of Gli transcription factors in the signal transduction pathway.

In this report, we show that a *Kif7* knockout mouse has defects in developmental patterning that are largely consistent with a loss of Gli3 repressor activity. Cos2 is required for full pathway activation [3, 5, 18], and we cannot exclude the possibility that Kif7 also has a role in Shh activation pathway and its loss contributes to the decreased ventral cell types in the neural tube. Both our in vitro studies and our in vivo analysis of Kif7's role indicate, though, that mouse Kif7 functions principally as a negative regulator of the Hh pathway, as was shown in zebrafish [6]. The importance of Kif7 in regulating Gli3 repressor activity is highlighted by the physical interaction between Kif7 and Gli3, and by the requirement for Kif7 in the proteolytic processing of Gli3. These results suggest that at least some functions of Kif7 are conserved with respect to those of Cos2 in *Drosophila* [5, 16, 17]. Our biochemical analysis of Gli3 processing indicates that Kif7 mutation leads to an approximately 2–3-fold reduction, but not a complete loss, of

Gli3 repressor formation. This residual Gli3 repressor activity seems to result in incomplete penetrance of the mutant phenotype. Most aspects of the *Kif7* mutant phenotype described here can be explained by reduced Gli3 repressor activity, with the apparent exception being the reduction in notochordal expression of Shh, which may reflect a distinct and unidentified role for Kif7. It is noteworthy in this regard that we found no evidence for diminished expression of Shh in other tissues such as the limb bud, indicating that Kif7 does not seem to have a general role in the upstream regulation of Shh expression.

Kif7 is important, but not absolutely required, for the efficient proteolytic processing of Gli3. This suggests that Kif7 plays a regulatory and not a catalytic role in the cleavage events and highlights what may be its fundamental role, as a mediator of Hh inhibition of Gli3 cleavage. Hh pathway activation is associated with translocation of Gli3 to the cilia, and the hierarchical requirement for Smo and Kif7 in this translocation points to a mechanistic explanation for how Kif7 regulates repressor formation. In the absence of Hh pathway activation, Gli3 is processed by the proteosome to produce repressor and Kif7 is required for this processing to occur efficiently, perhaps by mediating proper subcellular localization of Gli3. Upon exposure to Hh ligand, Smo enters the cilia and redirects the complex of Kif7 and Gli3 away from the subcellular site of Gli3 proteolysis, while at the same time mediating its accumulation at the tip of the cilia. This model mirrors many of the essential features of Cos2-mediated regulation of Ci repressor formation. The apparent parallel is strengthened by a recent study showing that Cos2 moves along microtubules in a Hh-dependent manner through its kinesin-like motor function and regulates Ci localization [28]. Ciliary localization of Kif7 is increased in a Hh-dependent manner and required for parallel accumulation of Gli2 and Gli3 at the tip of cilia. These similarities further support the idea that the Hh signal transduction mechanism is more conserved between flies and vertebrates than has been generally recognized.

Very recently, it was reported that mouse Fused interacts with Kif27 but not with Kif7 and plays an essential role in construction of the central pair of motile (9+2) cilia [29]. Kif7 and Kif27 seem to have arisen by a duplication event during evolution, whereas zebrafish does not contain an obvious Kif27 ortholog and a dual role for zebrafish Kif7 is suggested in Hh signaling and motile ciliogenesis [29]. Future analyses will address whether Kif27 plays a redundant role with Kif7 in Hh signaling or whether the two paralogs have evolved separate functions.

Experimental Procedures

Animals

Kif7$^{+/-}$ mice (see Figure S1) were backcrossed and maintained on C57BL/6 background. Intercrosses between heterozygous offspring were used to obtain *Kif7*$^{-/-}$ mice. For visualization of Hh pathway activation, *Kif7*$^{+/-}$ mice were crossed to *Ptch-LacZ*$^{+/-}$ (*Ptch*^{D11}) mice [8] and the *Ptch-LacZ*$^{+/-}$; *Kif7*$^{+/-}$ offspring were further crossed with *Kif7*$^{+/-}$ mice to generate *Ptch-LacZ*$^{+/-}$; *Kif7*$^{+/+}$ and *Ptch-LacZ*$^{+/-}$; *Kif7*$^{-/-}$ embryos. Genotyping of *Kif7* knockout mice was performed by PCR with primers directed against *neo* (5′-GCAGCGCATCGCCTTCTATCG-3′), exon 2 (5′-GGCGGGACCGACACTTTGGG-3′), and intron 2 (5′-CACCTGACATGGAGTGCTGACC-3′), which generates a 302 bp product in the WT and 197 bp product in the knockout allele. Noon of the day of vaginal plug detection was termed as embryonic day (E) 0.5. All animals were handled in accordance with protocols approved by the Genentech Institutional Animal Care and Use Committee. Mouse colonies were maintained in a barrier facility at Genentech, conforming to State of California legal and ethical standards of animal care.

Histology

For immunofluorescent staining, mouse embryos were fixed by immersion in 4% paraformaldehyde in phosphate-buffered saline and processed for paraffin sections at 10 μm. The antibodies used are as follows: rabbit anti-Shh monoclonal (clone 95.9, 2 μg/ml; Josman/Epitomics/Genentech), goat anti-Olig2 (1:500; Santa Cruz), mouse anti-Nkx2.2 (2.15 μg/ml; DSHB), mouse anti-Pax6 (1:5; DSHB), anti-FoxA2 (1:2,000; Abcam), and fluorescent secondary antibodies conjugated with Alexa 488, 555, or 647 (1:400; Invitrogen). Images were acquired on a confocal microscope LSM510 (Carl Zeiss). X-gal staining was performed according to standard methods. Skeletons from E15.5 embryos were prepared with Alcian blue and Alizarin red as described [30]. Whole-mount in situ hybridization was performed with digoxigenin-labeled riboprobes according to standard methods. The probes (*Gli1*, *Gremlin*, *HoxD13*, and *Shh*) were kind gifts from A. McMahon [31].

Biochemical and Molecular Analysis

For Gli3 immunoblot analysis, anterior portions of E10.5 embryos were homogenized in RIPA buffer (20 mM Tris-HCl, pH 7.5, 150 mM NaCl, 1% NP-40, 0.5% sodium deoxycholate, 0.1% SDS, 10 mM EDTA, 10 mM EGTA, Complete protease inhibitor cocktail (Roche), and phosphatase inhibitor cocktail [Sigma]). We confirmed that anterior and posterior portions of the embryo gave the same results. Twenty micrograms of protein was loaded in each lane, resolved by SDS-PAGE, transferred to PVDF membrane, and detected with ECL-plus reagent (GE Healthcare) with the use of Gli3N mAb (mouse monoclonal antibody against the N-terminal region of human Gli3, clone 6F5, 1:100; raised in Genentech) and ChemiBLOCKER (Millipore). Coimmunoprecipitation experiments and real-time qRT-PCR were carried out as described previously [32]. Human Kif7 (hKif7) cDNA was purchased from OriGene, Inc. (Rockville, MD).

Cell Culture and Primary Cilia Experiments

For the creation of the Kif7-GFP cell line, hKif7 with a C-terminal GFP tag was cloned into a Flp-In targeting vector pEF5-FRT-CT-lap [33] and integrated into NIH 3T3 Flp-In cells (Invitrogen). Cells were selected for Hygromycin resistance. One of the clones was chosen on the basis of low levels of GFP expression and responsiveness to Hh signaling. MEFs were prepared from E10.5–E13.5 embryos and cultured in 10% FBS containing DMEM, according to the standard protocol. Pooled nontargeting control, Sufu, and Gli3 siRNA was purchased from Dharmacon. MEFs were transfected with 100 nM siRNA and Dharmafect #4 (Dharmacon) and were incubated for 3 days followed by additional 24 hr incubation in 0.5% FBS-containing media. For primary cilia experiments, WT or *Kif7*$^{-/-}$ MEFs were plated at a density of 100,000, and Kif7-GFP cells were plated at a density of 15,000 cells per well of 8-well chamber slides. For Smo knockdown experiments, 20,000 Kif7-GFP cells were reverse-transfected with 100 nM pooled nontargeting or Smo siRNA and Dharmafect #4 in 8-well chamber slides. After 48 hr, the FBS was reduced to 0.5% to serum starve cells and induce the formation of primary cilia, and 200 ng/ml of Shh was added to induce the Hh pathway. Cells were then fixed with 4% PFA after an additional 24 hr and stained with mouse anti-acetylated tubulin (1:3000; Sigma) to visualize primary cilia, mouse anti-gamma tubulin (1:2,300; Sigma) to determine orientation of the primary cilia, chicken anti-GFP (1:1,000; Novus Biologicals) to visualize Kif7, and rabbit polyclonal anti-Gli3N (against the N-terminal region of human Gli3, rabbit 2676A, 3 μg/ml; Josman Labs/Genentech) or rabbit anti-Smo (rabbit 5928B, 3 μg/ml; Josman Labs/Genentech). Images were acquired with a Deltavision RT Deconvolution System (Applied Precision) and quantified with ImageJ software (http://rsbweb.nih.gov/ij/).

Supplemental Data

Supplemental Data include seven figures and can be found with this article online at http://www.cell.com/current-biology/supplemental/S0960-9822(09)01323-2.

Acknowledgments

We thank J. Hongo, K. Schroeder, N. Pal, S. Bheddah, L. Rangell, C. Callahan, Josman Labs, LLC (Napa, CA), and Epitomics, Inc. (Burlingame, CA) for help in generation of Gli3, Gli2, Shh, and Smo antibodies; M. Wong and C. Brown for making the antigens; J. Ernst and H. Li for octylated Shh; C. Lai for advice on primary cilia experiments; and J. Torres, J. Miller, and P. Jackson for pEF5-FRT-CT-lap vector. The Pax6 and Nkx2.2 antibodies developed by A. Kawakami and T. Jessell, respectively, were obtained from the Developmental Studies Hybridoma Bank developed under the

auspices of the National Institute of Child Health and Human Development and maintained by The University of Iowa, Department of Biological Sciences, Iowa City, IA 52242. We also thank M. Scott for use of the *Ptch*^{D11} mice and A. McMahon for in situ hybridization probes. *Kif7* knockout mice were produced in a collaboration between Genentech and Lexicon Pharmaceuticals, Inc. (The Woodlands, TX) to analyze the function of about 500 secreted and transmembrane proteins. M.E., D.W., X.W., J.-W.T., K.P., S.J.S, M.J.S., F.J.d.S., and A.S.P. are employees of Genentech, Inc.

Received: March 31, 2009
Revised: June 19, 2009
Accepted: June 22, 2009
Published online: July 9, 2009

References

1. Huangfu, D., and Anderson, K.V. (2006). Signaling from Smo to Ci/Gli: Conservation and divergence of Hedgehog pathways from Drosophila to vertebrates. Development *133*, 3–14.
2. Jiang, J., and Hui, C.C. (2008). Hedgehog signaling in development and cancer. Dev. Cell *15*, 801–812.
3. Lum, L., and Beachy, P.A. (2004). The Hedgehog response network: Sensors, switches, and routers. Science *304*, 1755–1759.
4. Varjosalo, M., Li, S.P., and Taipale, J. (2006). Divergence of hedgehog signal transduction mechanism between Drosophila and mammals. Dev. Cell *10*, 177–186.
5. Ingham, P.W., and McMahon, A.P. (2001). Hedgehog signaling in animal development: Paradigms and principles. Genes Dev. *15*, 3059–3087.
6. Tay, S.Y., Ingham, P.W., and Roy, S. (2005). A homologue of the Drosophila kinesin-like protein Costal2 regulates Hedgehog signal transduction in the vertebrate embryo. Development *132*, 625–634.
7. Hui, C.C., and Joyner, A.L. (1993). A mouse model of greig cephalopolysyndactyly syndrome: The extra-toesJ mutation contains an intragenic deletion of the Gli3 gene. Nat. Genet. *3*, 241–246.
8. Oro, A.E., and Higgins, K. (2003). Hair cycle regulation of Hedgehog signal reception. Dev. Biol. *255*, 238–248.
9. Jacob, J., and Briscoe, J. (2003). Gli proteins and the control of spinal-cord patterning. EMBO Rep. *4*, 761–765.
10. Niswander, L. (2003). Pattern formation: Old models out on a limb. Nat. Rev. Genet. *4*, 133–143.
11. Bai, C.B., Stephen, D., and Joyner, A.L. (2004). All mouse ventral spinal cord patterning by hedgehog is Gli dependent and involves an activator function of Gli3. Dev. Cell *6*, 103–115.
12. Wijgerde, M., McMahon, J.A., Rule, M., and McMahon, A.P. (2002). A direct requirement for Hedgehog signaling for normal specification of all ventral progenitor domains in the presumptive mammalian spinal cord. Genes Dev. *16*, 2849–2864.
13. Vokes, S.A., Ji, H., Wong, W.H., and McMahon, A.P. (2008). A genome-scale analysis of the cis-regulatory circuitry underlying sonic hedgehog-mediated patterning of the mammalian limb. Genes Dev. *22*, 2651–2663.
14. te Welscher, P., Zuniga, A., Kuijper, S., Drenth, T., Goedemans, H.J., Meijlink, F., and Zeller, R. (2002). Progression of vertebrate limb development through SHH-mediated counteraction of GLI3. Science *298*, 827–830.
15. Wang, B., Fallon, J.F., and Beachy, P.A. (2000). Hedgehog-regulated processing of Gli3 produces an anterior/posterior repressor gradient in the developing vertebrate limb. Cell *100*, 423–434.
16. Sisson, J.C., Ho, K.S., Suyama, K., and Scott, M.P. (1997). Costal2, a novel kinesin-related protein in the Hedgehog signaling pathway. Cell *90*, 235–245.
17. Wang, Q.T., and Holmgren, R.A. (1999). The subcellular localization and activity of Drosophila cubitus interruptus are regulated at multiple levels. Development *126*, 5097–5106.
18. Wang, G., Amanai, K., Wang, B., and Jiang, J. (2000). Interactions with Costal2 and suppressor of fused regulate nuclear translocation and activity of cubitus interruptus. Genes Dev. *14*, 2893–2905.
19. Stegman, M.A., Vallance, J.E., Elangovan, G., Sosinski, J., Cheng, Y., and Robbins, D.J. (2000). Identification of a tetrameric hedgehog signaling complex. J. Biol. Chem. *275*, 21809–21812.
20. Jia, J., Tong, C., and Jiang, J. (2003). Smoothened transduces Hedgehog signal by physically interacting with Costal2/Fused complex through its C-terminal tail. Genes Dev. *17*, 2709–2720.
21. Lum, L., Zhang, C., Oh, S., Mann, R.K., von Kessler, D.P., Taipale, J., Weis-Garcia, F., Gong, R., Wang, B., and Beachy, P.A. (2003). Hedgehog signal transduction via Smoothened association with a cytoplasmic complex scaffolded by the atypical kinesin, Costal-2. Mol. Cell *12*, 1261–1274.
22. Corbit, K.C., Aanstad, P., Singla, V., Norman, A.R., Stainier, D.Y., and Reiter, J.F. (2005). Vertebrate Smoothened functions at the primary cilium. Nature *437*, 1018–1021.
23. Haycraft, C.J., Banizs, B., Aydin-Son, Y., Zhang, Q., Michaud, E.J., and Yoder, B.K. (2005). Gli2 and Gli3 localize to cilia and require the intraflagellar transport protein polaris for processing and function. PLoS Genet. *1*, e53.
24. Huangfu, D., and Anderson, K.V. (2005). Cilia and Hedgehog responsiveness in the mouse. Proc. Natl. Acad. Sci. USA *102*, 11325–11330.
25. May, S.R., Ashique, A.M., Karlen, M., Wang, B., Shen, Y., Zarbalis, K., Reiter, J., Ericson, J., and Peterson, A.S. (2005). Loss of the retrograde motor for IFT disrupts localization of Smo to cilia and prevents the expression of both activator and repressor functions of Gli. Dev. Biol. *287*, 378–389.
26. Liu, A., Wang, B., and Niswander, L.A. (2005). Mouse intraflagellar transport proteins regulate both the activator and repressor functions of Gli transcription factors. Development *132*, 3103–3111.
27. Jia, J., Kolterud, A., Zeng, H., Hoover, A., Teglund, S., Toftgard, R., and Liu, A. (2009). Suppressor of Fused inhibits mammalian Hedgehog signaling in the absence of cilia. Dev. Biol. *330*, 452–460.
28. Farzan, S.F., Ascano, M., Ogden, S.K., Sanial, M., Brigui, A., Plessis, A., and Robbins, D.J. (2008). Costal2 functions as a kinesin-like protein in the hedgehog signal transduction pathway. Curr. Biol. *18*, 1215–1220.
29. Wilson, C.W., Nguyen, C.T., Chen, M.H., Yang, J.H., Gacayan, R., Huang, J., Chen, J.N., and Chuang, P.T. (2009). Fused has evolved divergent roles in vertebrate Hedgehog signalling and motile ciliogenesis. Nature *459*, 98–102.
30. Solloway, M.J., Dudley, A.T., Bikoff, E.K., Lyons, K.M., Hogan, B.L., and Robertson, E.J. (1998). Mice lacking Bmp6 function. Dev. Genet. *22*, 321–339.
31. Lewis, P.M., Dunn, M.P., McMahon, J.A., Logan, M., Martin, J.F., St-Jacques, B., and McMahon, A.P. (2001). Cholesterol modification of sonic hedgehog is required for long-range signaling activity and effective modulation of signaling by Ptc1. Cell *105*, 599–612.
32. Evangelista, M., Lim, T.Y., Lee, J., Parker, L., Ashique, A., Peterson, A.S., Ye, W., Davis, D.P., and de Sauvage, F.J. (2008). Kinome siRNA screen identifies regulators of ciliogenesis and hedgehog signal transduction. Sci. Signal. *1*, ra7.
33. Torres, J.Z., Miller, J.J., and Jackson, P.K. (2009). High-throughput generation of tagged stable cell lines for proteomic analysis. Proteomics *9*, 2888–2891.